Jurnal Teknik Mesin Mechanical Xplore (JTMMX)
Journal homepage: https://journal.ubpkarawang.ac.id/index.php/JTMMX

Original Article

Design of a Sintering Machine for 316 L Material Products from 3D Printing for Product Design Engineering Laboratory

Dinny Indrian[1], Erfanli M Hutasoit[1], Adi S Pradipta[1],

[1]Department of Design Engineering, Politeknik Manufaktur Bandung, Bandung, 40135, West Java, Indonesia

ARTICLE INFO

Article history:
Received 4 Nov. 2025
Received in revised form
23 Jan. 2026
Accepted 9 Feb 2026
Available online 28 Feb 2026

Keywords:
Sintering machine
316 L stainless steel
Additive manufacturing
Design methodology
VDI 2222

ABSTRACT

The increasing demand for high-performance metal components in additive manufacturing necessitates effective post-processing methods to enhance material density and mechanical properties. This study presents the design of a compact laboratory-scale sintering machine for 316 L stainless steel components fabricated using fused-filament fabrication (FFF). The design process adopted a simplified VDI 2222 methodology encompassing planning, conceptual design, and detailed design stages. Functional decomposition and systematic evaluation of the alternative design concepts were conducted using the VDI 2225-based assessment method, leading to the selection of the optimal configuration. Thermal analysis and radiation-based simulations demonstrated that the proposed system is capable of achieving the required sintering temperature range for 316 L stainless steel (approximately 1100–1300 °C) with a stable heat distribution. Structural analysis further confirmed that all critical components operated within acceptable safety limits, with safety factors exceeding the standard design criteria. Overall, the proposed design provides a technically feasible and safe solution for laboratory-scale sintering, supporting research and prototyping in metal additive manufacturing.

*Corresponding author.
E-mail address: dinny@polman-bandung.ac.id (D. Indrian)
Peer review under the responsibility of Editorial Board of Jurnal Teknik Mesin Mechanical Xplore (JTMMX)

1. Introduction

The manufacturing industry is experiencing increasingly fierce competition driven by rapid technological advancements and the demand for products with high economic value, time efficiency, and design flexibility. Conventional manufacturing methods often face limitations when producing complex geometries or working with diverse material combinations [1]. Additive manufacturing (AM), commonly known as 3D printing, addresses these challenges by enabling the layer-by-layer fabrication of three-dimensional objects directly from digital models [2]. Among its various technologies, metal AM has gained significant attention for producing high-performance components with intricate designs [3, 4], making it particularly attractive for rapid prototyping, customized production, and functional part development in both industrial and academic environments.

In metal AM processes, a 316 L stainless steel filament comprising fine metal powder bound by polymer binders is widely used [5, 6]. Although this allows extrusion-based printing, the as-printed parts exhibit mechanical properties closer to those of polymers than fully dense metals

https://doi.org/10.36805/cy835n03

owing to the presence of binders and residual porosity [7-9]. Consequently, post-processing is required to remove binders, increase densification, and improve the mechanical properties to match those of conventionally manufactured components [10, 11]. Previous studies have consistently demonstrated that thermal post-processing significantly influences the microstructure, mechanical properties, and corrosion resistance of 316 L stainless steel [9].

Recent research on sinter-based extrusion additive manufacturing indicates that the final density, microstructure, and mechanical behavior of 316 L parts are strongly governed by sintering conditions, including temperature uniformity, holding time, and atmosphere control [6]. Sintering is a thermal process that consolidates powdered or binder-containing materials through atomic diffusion, thereby reducing porosity and enhancing material density [12, 13]. For 316 L stainless steel, the optimal sintering temperature ranges from 1300 to 1350 °C under controlled atmosphere to prevent oxidation [14, 15]. However, commercial sintering systems are typically designed for large-scale production, featuring complex mechanisms and high costs that limit their use in laboratories and educational settings [16-18]. Such systems are often oversized and economically impractical, which restricts their flexibility for experimental studies and prototyping.

Most previous studies have emphasized material characterization and optimization of sintering parameters for 316 L using industrial-scale systems [7, 8, 10, 11, 19]. While these studies provide valuable insights into temperature ranges, holding times, and atmospheric control, they largely assume access to advanced industrial furnaces. Therefore, there is a research gap in developing compact, safe, and cost-effective sintering systems suitable for laboratory-scale applications that support research and education in metal AM [16-18]. In particular, limited attention has been paid to design-oriented studies that systematically develop lab-scale sintering equipment tailored for FFF-based metal printing [15, 17, 19].

To address this gap, in this study, we propose the design of a compact sintering furnace tailored for laboratory-scale use. The novelty of this work lies in the adaptation of the VDI 2222 design methodology into a simplified and application-oriented framework for developing a sintering system that balances thermal performance, structural integrity, operational safety, and manufacturability. The design process encompasses planning, conceptualization, embodiment, and finalization stages, as illustrated in Figure 1. The proposed system is designed to achieve the required sintering temperature range for 316 L stainless steel while maintaining suitability for academic and prototyping environments. The design is further evaluated through thermal and structural analyses to ensure its feasibility and reliability, thereby establishing a clear foundation for the results and discussion presented in the subsequent sections.

2. Methods

The sintering machine designed in this study adopts and simplifies the Verein Deutscher Ingenieure (VDI) 2222 methodology, which provides a systematic framework for the conceptualization and development of technical products [16]. This methodology was selected because of its structured approach in translating functional requirements into engineering design solutions, making it particularly suitable for early-stage product development in mechanical and manufacturing engineering.

VDI 2222 emphasizes functional decomposition, systematic generation and evaluation of alternative solutions, and iterative refinement. These characteristics are essential for the development of a laboratory-scale sintering system that must balance thermal performance, operational safety, manufacturability, and ease of use. Compared with more generic design approaches, VDI 2222 offers clearer guidance in identifying and evaluating multiple functional configurations before progressing to detailed engineering design.

For the scope of this research, the methodology was adapted by focusing on the planning, conceptual design, and detailed design stages. Manufacturing planning and experimental validation are defined as future work. This simplification retains the core principles of VDI 2222 while ensuring that the method remains practical and aligned with the objectives of a design-oriented study.

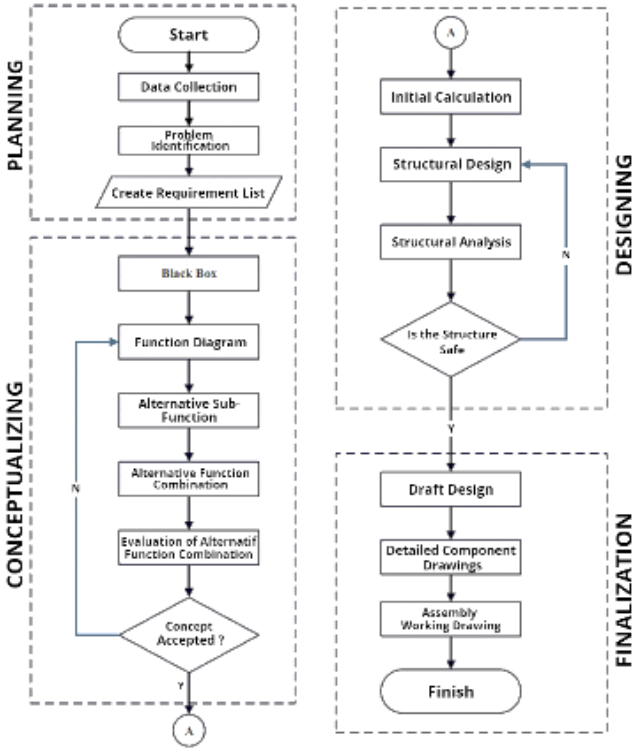

Figure 1. Research methodology based on the adapted VDI 2222 design framework

To systematically implement this methodology, the following sections detail the stepwise approach adopted in this study, covering the planning, conceptualization, and detailed design stages. This structure allows for clear traceability from the identified requirements to the final engineering solutions. The applied framework focuses on the planning, conceptual design, and detailed design stages.

2.1. Planning

The planning stage aims to establish the design boundaries and technical requirements of the sintering machine. This stage begins with the identification of the target material processed in this study, namely, a 316 L stainless steel filament used in metal FFF technology. Relevant material characteristics, processing behavior, and post-printing requirements were reviewed from the literature and existing industrial practices.

Process constraints related to the sintering temperature, holding time, atmosphere control, and laboratory safety considerations were identified through a literature survey and benchmarking of commercial and research-scale sintering systems. Additionally, constraints related to the part dimensions were derived from the build volume of the available metal FFF printer used in this study.

The outcomes of this stage are not numerical results but a structured list of technical and operational requirements that serve as the design input for the conceptual design stage. These requirements are summarized and reported in the Results section.

2.2. Conceptualizing

Functional modeling was conducted to translate the planning-stage requirements into technical functions that define the operational structure of the sintering machine. The process began with the development of a black-box model to establish system boundaries by identifying the required inputs, internal

processes, and expected outputs. This was followed by a glass-box model, in which the internal processes were further decomposed into individual functional elements, allowing a clearer understanding of the interactions between subsystems. This functional modeling approach ensures traceability between the defined requirements and the proposed technical solutions and provides a systematic foundation for subsequent concept generation.

Based on the functional decomposition, the sintering machine was divided into several primary functional elements for which multiple sub-function alternatives were generated to explore different technical solutions and design trade-offs. These alternatives were evaluated using criteria relevant to laboratory-scale equipment, including functional performance, operational safety, manufacturability, ease of assembly, maintenance considerations, and the use of standard components. To integrate the selected sub-functions into feasible system-level designs, several alternative function combinations (AFCs) were formulated. An objective selection process was then carried out using a weighted evaluation method adapted from the VDI 2225 guideline, in which each evaluation criterion was assigned a relative importance weight and each alternative was rated accordingly. This systematic assessment resulted in a ranked comparison of the alternative concepts, enabling the selection of the most suitable configuration for further development; detailed evaluation results and the selected concept are presented in the Results section.

2.3. Designing

The selected conceptual design was further developed through detailed engineering analysis. Thermal analysis was conducted using analytical heat transfer equations, with particular emphasis on radiation heat transfer, to estimate heating requirements and system performance. In addition, calculations were performed to determine the number of heating elements and their required power to achieve the target sintering temperature for 316 L stainless steel. Six heating elements were selected, and their power distribution was optimized based on thermal analysis to ensure a uniform temperature distribution within the sintering chamber. Simplified thermal simulations were conducted to verify the effectiveness of the heating and insulation configuration and confirm that the design met the required thermal performance requirements.

A structural strength analysis was also performed on critical components to ensure mechanical safety under static loading conditions. These analyses provide technical validation of the selected concept prior to fabrication, whereas detailed numerical results and simulation outcomes are reported separately in the Results section.

3. Results and Discussions

3.1. Results of planning stage

The planning stage resulted in the definition of material selection, process constraints, and technical requirements for the sintering machine. The primary material processed in this study is a 316 L stainless steel filament, which is widely used in metal fused-filament fabrication (FFF) owing to its good corrosion resistance, satisfactory mechanical properties after sintering, and relatively lower cost compared to other metal alloys. These characteristics make 316 L stainless steel suitable for both research and educational applications in metal additive manufacturing.

Table 1. Comparison of 3D printing process parameters between 316 L and PLA filaments

3D Printing Process Parameters	316 L	PLA
Nozzle Temperature	230–250ºC / 446–482ºF	210–230ºC / 410–446ºF
Bed Temperature	90–120ºC / 194–248ºF	50–70ºC / 122–158ºF
Print Speed	15–50 mm/s	40–80 mm/s
Density	7,850 kg/m³	1,248 kg/m³

A comparison of the printing parameters between 316 L and PLA filaments, as presented in Table 1, shows that extrusion-based processing parameters, such as nozzle and bed temperatures, are comparable, whereas significant differences exist in material density and printing speed. Although the printing process is similar to that of polymer-based filaments, the as-printed 316 L components still exhibit polymer-like mechanical behavior because of the presence of binders and internal porosity. This result confirms the necessity of a sintering process to achieve metallic density and mechanical performance.

The printed specimens used in this study were produced using a MakerBot Method X 3D printer with a maximum build volume of 190 mm × 190 mm × 196 mm. Consequently, the sintering chamber was designed to accommodate parts within these dimensional limits, resulting in a chamber size of 250 mm × 250 mm × 250 mm to provide sufficient clearance and uniform heat exposure.

Based on the literature, the sintering of stainless steel is typically conducted at 70–90% of its melting temperature, corresponding to a temperature range of 1101–1291°C for 316 L stainless steel, with holding times between 30 and 60 min. This process requires a controlled, oxygen-free environment to prevent oxidation. Previous studies have indicated that nitrogen gas provides a stable and effective inert atmosphere compared to vacuum or alternative inert gases.

Based on this analysis, the key planning outcomes are summarized as follows:

- The printed parts underwent binder removal and porosity reduction through sintering.
- Improvement of the sintering process to approach the mechanical properties of conventionally manufactured 316 L components is required.
- The sintering machine should be safe, ergonomic, and suitable for laboratory operations.

These considerations are translated into a list of technical and operational requirements, as summarized in Table 2.

Table 2. List of Requirements

No	Main Requirements	Description
1	Product temperature	1,101°C–1,291°C
2	Sintering duration	30–60 minutes
3	Sintering chamber dimensions	250 mm × 250 mm × 250 mm
4	Atmosphere	Nitrogen (non-vacuum)
5	Temperature sensor	Type-S thermocouple

3.2. Results of conceptual design stage

3.2.1. Functional modeling

The conceptual design stage resulted in the development of a functional model using black-box and glass-box representations (Figure 2). The black-box model defines the relationship between system inputs (electrical energy, nitrogen gas, and raw printed parts), internal processes (heating, thermal insulation, and temperature control), and outputs (sintered metal components). The glass box further decomposes these processes into detailed functional elements, ensuring traceability between requirements and design solutions.

3.2.2. Alternative function generation and evaluation

The conceptual design stage identified seven primary functional elements of the sintering machine: frame, refractory structure, heating system, thermal insulation, temperature sensing, door system, and temperature control. Multiple sub-function alternatives were generated for each element to explore different technical solutions and design trade-offs. These alternatives were evaluated based on criteria relevant to laboratory-scale applications, including functional performance, safety, manufacturability, ease of assembly, maintenance requirements, and the utilization of standard components (Table 3).

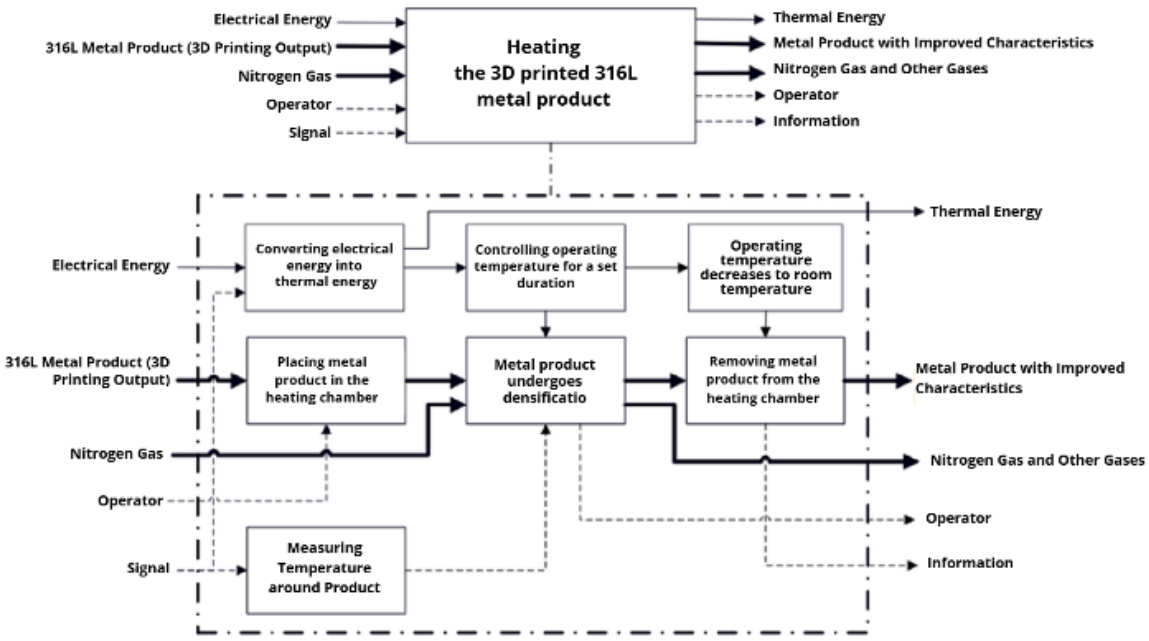

Figure 2. Functional modeling of the sintering machine using black box and glass box representations to define system boundaries, input–output relationships, and internal functional decomposition

Table 3. Comparison of functional elements and design alternatives for laboratory-scale sintering machine.

Function	Alternative	Advantages	Disadvantages
Frame Function	Box (A1)	– Easy to manufacture/assemble- Easy maintenance	– Tend to be heavier due to more components- More components to assemble
	Cylinder (A2)	– Lighter construction- Fewer components	– Difficult to manufacture/assemble- Requires special maintenance to maintain shape stability
Refractory Function	Thermal Resistant Brick (B1)	– High durability- Dimensional stability- Good mechanical strength	– More complex installation- Lower thermal insulation
	Layered Ceramic Fiber Board (B2)	– Good thermal insulation- Lightweight and easy to install- Resistant to rapid temperature changes	– Physically fragile, prone to cracking or breaking under mechanical stress- Requires special care as fiber dust can be a health hazard
Heating Function	U-Shape (C1)	– Easy to install in large spaces- Durable	– Must be assembled vertically- If one side is damaged, replacement is required
	Rod Type (C2)	– Can be installed horizontally or vertically- Easy to replace if damaged	– Less uniform heat distribution in wide spaces
	Circular (C3)	– Even heat distribution	– Difficult to repair or replace- Requires dedicated space
Heat Insulator Function	Ceramic Fiber Blanket (D1)	– Lightweight, easy to cut and fit- High heat resistance up to 1300°C	– Fragile under excessive mechanical pressure- Requires special tools for safe assembly to prevent fiber exposure
	Layered Ceramic Fiber Board (D2)	– No special maintenance required- Affordable price	– Heat resistance only up to 300°C- Prone to flaking, leading to quality

Function	Alternative	Advantages	Disadvantages
			degradation
Temperature Sensor Function	Single Point (E1)	– Simple and economical- Easy installation	– Less accurate than dual-point sensor- Requires regular functional checks
	Dual Point (E2)	– More accurate readings- Easier data acquisition	– More expensive and requires calibration- Requires more installation space
Door Function	Four-Point Locking (F1)	– Stronger and tighter locking- Even load distribution	– Requires more components- longer installation time
	Hinge + Latch (F2)	– Fewer and standard components- Faster installation/locking	– Must ensure tight sealing- uneven load distribution
Temperature Control Function	Digital Display (G1)	– Flexible adjustments- More features	– More expensive- Display limitations
	Analog (G2)	– Simple and stable- Lower cost	– Limited adjustment options- Minimal information provided

To integrate these alternatives into feasible system-level designs, three alternative function combinations (AFC1–AFC3) were formulated, as summarized in Table 4. Each combination represents a specific configuration of sub-functions selected from the morphological chart. An objective selection process was conducted using a weighted evaluation method adapted from the VDI 2225 design guidelines, in which each criterion was assigned a weight according to its relative importance in meeting the design objectives.

Table 4. Alternative function combinations (AFC1–AFC3) for system-level design evaluation

Sub Functions	Alternative Function Part		
	Alternative Function Combination 1 (AFK1)	Alternative Function Combination 1 (AFK2)	Alternative Function Combination 3 (AFK3)
Frame	A1	A1	A2
Refractory	B1	B2	B1
Heating	C2	C1	C3
Heat Insulator	D1	D2	D1
Temperature Sensor	E1	E1	E2
Door System	F2	F1	F2
Temperature Control	G1	G2	G1

Table 5 indicate that AFC1 achieved the highest overall score of 355 points (89%), marginally outperforming AFC2 (350 points, 88%), and clearly exceeding AFC3 (305 points, 76**%**). Although the numerical difference between AFC1 and AFC2 is relatively small, AFC1 demonstrates better performance across the most critical criteria, particularly functional achievement, operational safety, and compatibility with standard components. These aspects are essential for ensuring reliable operation, ease of maintenance, and safe use in academic laboratory environments. Consequently, AFC1 was selected as the most suitable configuration for further development

As illustrated in Figure 3, the selected design adopts a box-type frame that provides sufficient structural rigidity and simplifies the assembly and maintenance. The refractory chamber is constructed from thermal-resistant bricks to ensure dimensional stability at elevated temperatures, while silicon carbide rod heating elements are employed for their high thermal efficiency and durability. Ceramic fiber insulation is used to reduce heat loss and improve energy efficiency. Temperature monitoring and control are achieved

using thermocouples and a digital control system, enabling precise regulation of the sintering process. A hinged door with latch locking ensures safe operation and convenient handling of the workpieces. Overall, the selected configuration satisfies the functional, operational, and safety requirements, as confirmed by the VDI 2225-based evaluation.

Table 5. Weighted evaluation results of alternative function combinations using the VDI 2225 method.

Evaluation Aspect	Weight (%)	AFC1	AFC2	AFC3	Ideal Value
Functional Achievement	20	4 | 80	4 | 80	3 | 60	4 | 80
Construction	10	4 | 40	3 | 30	4 | 40	4 | 40
Maintenance	15	3 | 45	4 | 60	3 | 45	4 | 60
Assembly	20	3 | 60	3 | 60	2 | 40	4 | 80
Operation	15	4 | 60	4 | 60	4 | 60	4 | 60
Component Manufacturing	10	4 | 40	3 | 30	3 | 30	4 | 40
Use of Standard Components	10	3 | 30	3 | 30	3 | 30	4 | 40
Total Score	100	355	350	305	400
Percentage (%)	100	89	88	76	100

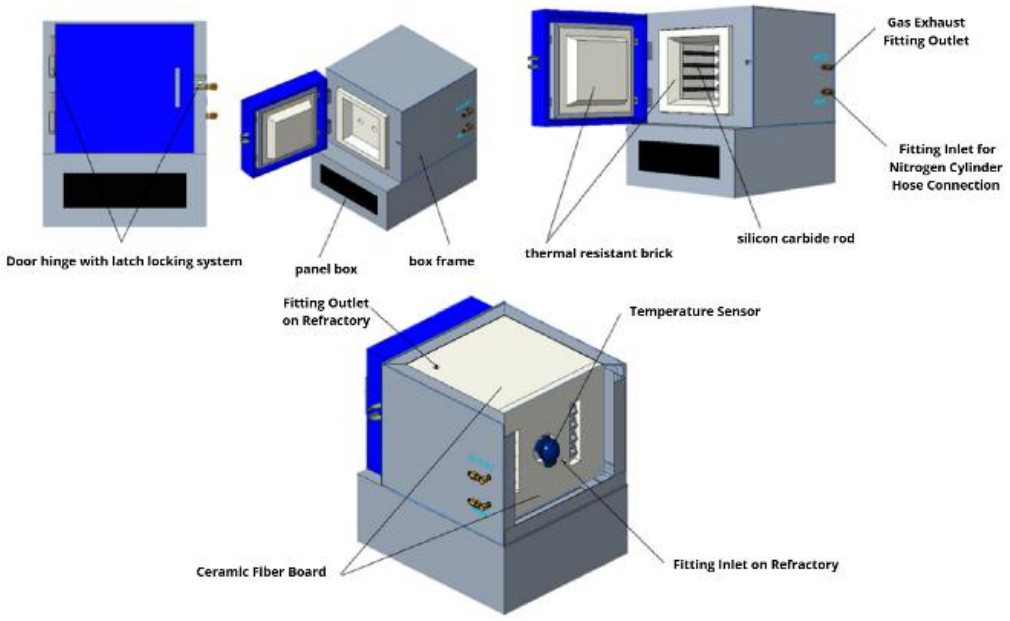

Figure 3. Optimal alternative function combination (AFC1) configuration of the laboratory-scale sintering furnace based on VDI 2225 evaluation.

3.3. Results of detailed design and thermal analysis

The selected concept was translated into a detailed engineering design through analytical calculations and thermal simulations. Heat transfer calculations based on radiation principles were performed to estimate the required heating power, total heat input, and heating time. At elevated operating temperatures exceeding 1000°C, thermal radiation becomes the dominant heat transfer mechanism compared to convection and conduction. The analytical formulation applied in this study follows classical radiation heat transfer theory, which relates heat exchange to surface emissivity, temperature difference, and geometric configuration. This approach is widely adopted in furnace and high-temperature chamber designs to obtain reliable first-order thermal performance estimations [20, 21].

Based on the calculated heat requirements, the number of heating elements and their individual power ratings were determined to ensure that the sintering chamber could reach and maintain the target temperature

range for 316 L stainless steel. Six heating elements with an optimized power distribution were selected to achieve uniform heating throughout the chamber. These calculations verified that the heating system satisfied the thermal requirements identified in the planning stage.

The results, summarized in Table 6, indicate that six heating elements with a total heat transfer rate of approximately 53.7 kW are sufficient to raise the product temperature to the sintering range within an acceptable time frame.

Table 6. Thermal design parameters and heating requirements of laboratory-scale sintering furnace.

Parameter	Value	Unit
Product surface area (A)	0.22116	m^2
Product volume (V)	7.0756×10^{-3}	m^3
Product mass (m)	55.543	kg
Radiative heat transfer rate (Q)	52,717.488	W
Total heat required (Q_{total})	59,946.3	kJ
Heating time (t)	19.854	min
Heat transfer rate per element ($Q_{element}$)	8,953.539	W
Total heat transfer rate for 6 elements	53,721.234	W
Time for heating elements to reach operating temperature	18.119	min

Radiation simulations were conducted using a simplified geometric model to evaluate the temperature distribution within the chamber. The simulation results (Figure 4) show that the product temperature reached 1114–1287 °C, which lies within the target sintering temperature range for 316 L stainless steel. This confirms that the proposed heating configuration and insulation strategy can achieve the desired thermal performance. This confirms that the analytical calculations and heating configuration are consistent and capable of achieving the required thermal performance, linking the methodology's "Designing" stage directly to the results [20, 21].

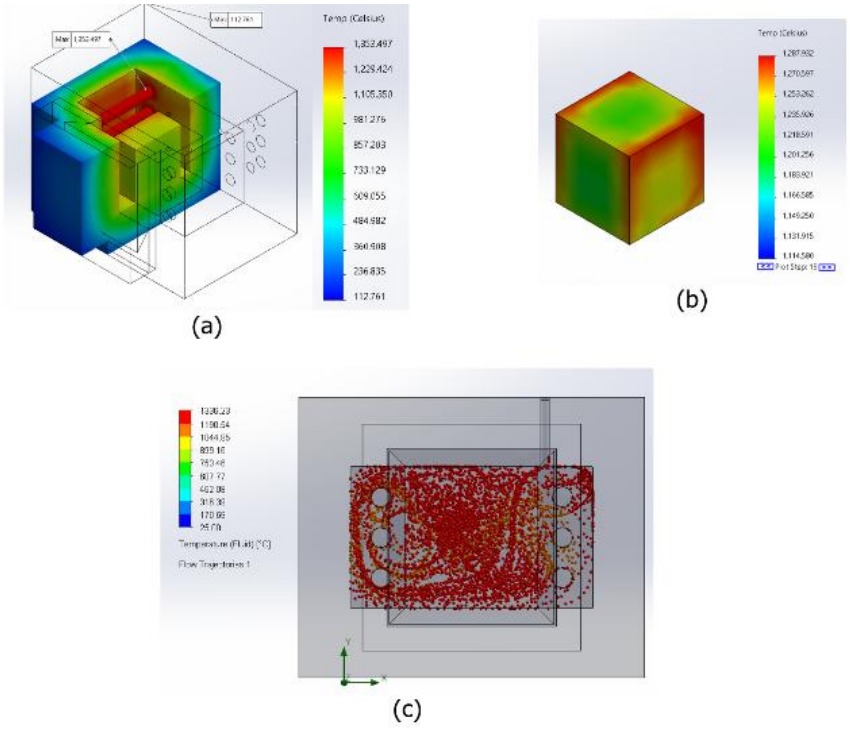

Figure 4. Thermal simulation results showing temperature distribution in (a) furnace components, (b) a 316 L workpiece, and (c) nitrogen gas within the sintering chamber.

The analysis also highlights the importance of balancing the heating element efficiency, product thermal properties, and refractory insulation. Proper coordination of these parameters ensures uniform heat distribution and stable sintering conditions, which are critical for achieving consistent material densification.

3.4. Structural strength and discussion

A structural analysis was performed to verify the mechanical safety of the sintering machine under static loading conditions. The frame, hinge, and hinge weld were identified as critical components and analyzed accordingly. The results, summarized in Table 7, show safety factors ranging from 1.958 to 52.72.

Table 7. Structural strength analysis results and safety factors of critical components under static loading

Component	Area	Total Stress (MPa)	Material & Re (MPa)	Safety Factor
Frame	Front	150.636	St.50 (E295), Re = 295	1.958
	Side	130.582	St.50 (E295), Re = 295	2.259
	Vertical	5.596	St.50 (E295), Re = 295	52.72
Hinge	—	12.533	Mild Steel S235, Re = 235	18.751
Hinge weld	—	3.322	Equivalent Re = 160	48.164

The minimum safety factor was observed in the front section of the frame (1.958), which represents the most critical structural region because of its direct exposure to operational loads and geometric constraints. Although this was the lowest value, it remained above the commonly accepted threshold of 1.5 for static steel structures, thereby satisfying standard mechanical design criteria [22]. This margin is considered adequate to accommodate uncertainties related to material variability, fabrication imperfections, and operational loading fluctuations [22, 23].

In contrast, the side and vertical sections of the frame exhibited higher safety factors (2.259 and 52.72, respectively), indicating a nonuniform stress distribution across the structure. The significantly high safety factor in the vertical section suggests that this region is overdesigned, which, while beneficial for safety, may indicate potential for material optimization and weight reduction.

Similarly, the hinge and hinge weld components demonstrate high safety factors of 18.751 and 48.164, respectively, confirming that these joints have sufficient strength to withstand repeated operational loading without the risk of mechanical failure [20-22]. However, such high margins may also imply conservative design assumptions that could be refined in future iterations to improve material efficiency without compromising structural reliability.

Overall, the structural analysis confirms that the proposed design meets the mechanical safety requirements for laboratory-scale operations. Furthermore, the variation in safety factors across components highlights opportunities for design optimization, particularly in reducing excessive material usage in low-stress regions while maintaining adequate safety margins in critical load-bearing areas.

3.5. Final design outcome and discussion

The final outcome of this research is a complete draft design for a compact sintering furnace optimized for laboratory use (Figure 5). The proposed system successfully integrates validated thermal performance with sufficient structural strength while maintaining operational simplicity and safety for non-industrial users. By adopting an adapted VDI 2222-based design approach, this study establishes a systematic framework for developing a laboratory-scale sintering machine capable of processing 316 L stainless steel components fabricated using fused-filament fabrication (FFF). The design feasibility is supported by

analytical calculations and numerical simulations, confirming that the furnace satisfies the key thermal and mechanical requirements [20-22]. However, because the present work is limited to design validation through modeling, further experimental investigation and performance testing are strongly recommended to verify operational reliability and sintering effectiveness under real laboratory conditions. Such validation is essential to ensure consistent production quality and to strengthen the practical applicability of the proposed system.

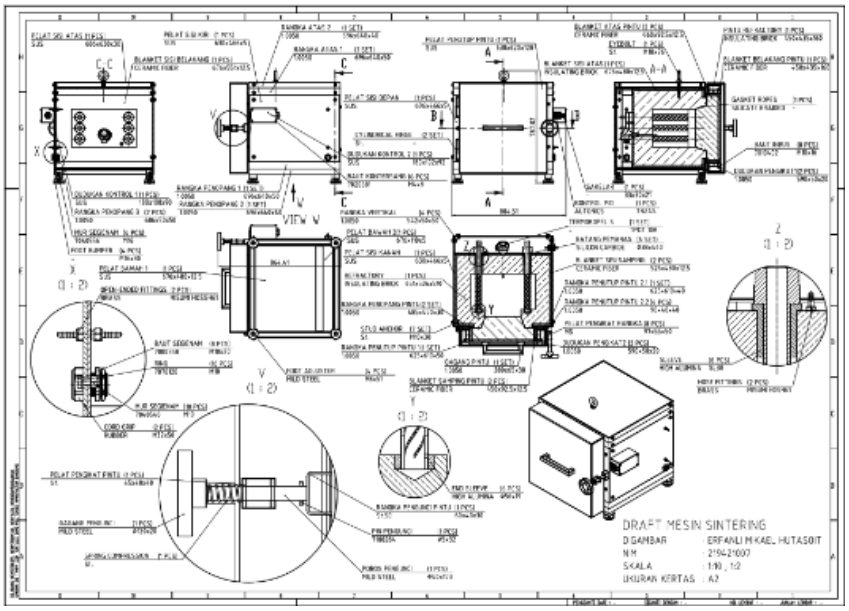

Figure 5. Draft design of the proposed compact sintering furnace for laboratory-scale metal FFF applications.

4. Conclusions

This study presents the systematic design of a compact sintering machine for laboratory-scale processing of 316 L stainless steel components fabricated using fused-filament fabrication (FFF) metal printing. By adapting and simplifying the VDI 2222 design methodology and applying a VDI 2225-based evaluation approach, a structured and objective framework was established to translate functional requirements into an optimized engineering design. The design process resulted in the identification and evaluation of multiple functional alternatives, from which the optimal configuration (AFC1) was selected based on quantitative assessment criteria. The selected design integrates a box-type structural frame, a thermal-resistant brick refractory, silicon carbide rod heating elements, ceramic fiber insulation, digital temperature control, and a nitrogen-based inert atmosphere system. Analytical calculations and thermal simulations confirmed that the proposed configuration can achieve the required sintering temperature range for 316 L stainless steel (approximately 1100–1300 °C) with stable heat distribution, whereas structural analysis demonstrated that all critical components satisfied safety requirements, with safety factors exceeding commonly accepted design limits for static loading conditions. The results indicate that the proposed sintering machine fulfills key functional, operational, and safety requirements for use in academic and prototyping environments. Compared with prior studies that primarily focused on material characterization using industrial-scale sintering systems, this work presents a design-oriented laboratory-scale framework that integrates functional decomposition, alternative evaluation, and simulation-based verification. Overall, the findings confirmed that the proposed design successfully achieved its objective of developing a compact, safe, and thermally reliable sintering system suitable for laboratory-scale metal FFF applications. Nevertheless, this study was limited to analytical calculations and numerical simulations; therefore, future work should include prototype fabrication, experimental validation of thermal performance,

evaluation of sintered-part density and mechanical properties, and long-term operational testing to further establish the practical reliability and applicability of the proposed design.

Author's Declaration

Authors' contributions and responsibilities

Author 1 conceived the idea and supervised the research as the principal investigator. Author 2 was responsible for the mechanical design, system fabrication, and technical testing. Author 3 contributed to the material selection, sintering process, and analysis of the metallurgical properties. All authors discussed the results, contributed to data interpretation, and approved the final manuscript.

Acknowledgment

The authors would like to thank the Mechanical Design and Manufacturing Laboratory Unit, Department of Manufacturing Design Engineering, Politeknik Manufaktur Bandung, for providing the laboratory facilities and technical assistance during this research.

Availability of data and materials

All data are available from the corresponding author.

Competing interests

The authors declare no conflicts of interest.

References

[1] S. A. Nugroho and A. A. Magriyanti, "Perkembangan Teknologi Dalam Proses Percetakan Tiga Dimensi dan Aplikasinya," *Jurnal Ilmiah Komputer Grafis,* vol. 8, no. 1, pp. 64–69, 2020. doi: https://doi.org/10.51903/pixel.v13i1.194

[2] B. Redwood, F. Schoffer, and B. Garret, *The 3D Printing Handbook: Technologies, Design and Applications*. Amsterdam, Netherlands Coers and Roest, 2017.

[3] C. K. Chua and K. F. Leong, *3D Printing and Additive Manufacturing*. WORLD SCIENTIFIC, 2016, p. 456.

[4] T. DebRoy, H. L. Wei, J. S. Zuback, T. Mukherjee, J. W. Elmer, J. O. Milewski, A. M. Beese, A. Wilson-Heid, A. De, and W. Zhang, "Additive manufacturing of metallic components – Process, structure and properties," *Progress in Materials Science,* vol. 92, pp. 112-224, 2018/03/01/ 2018. doi: https://doi.org/10.1016/j.pmatsci.2017.10.001

[5] Markforged. (2023, Dec. 2024). *Metal 3D Printing with 316 L Stainless Steel*. Available: https://markforged.com/materials/metals/316l-stainless-steel

[6] R. Santamaria, M. Salasi, S. Bakhtiari, G. Leadbeater, M. Iannuzzi, and M. Z. Quadir, "Microstructure and mechanical behaviour of 316L stainless steel produced using sinter-based extrusion additive manufacturing," *Journal of Materials Science,* vol. 57, no. 21, pp. 9646-9662, 2022/06/01 2022. doi: https://doi.org/10.1007/s10853-021-06828-8

[7] M. A. Wagner, J. Engel, A. Hadian, F. Clemens, M. Rodriguez-Arbaizar, E. Carreño-Morelli, J. M. Wheeler, and R. Spolenak, "Filament extrusion-based additive manufacturing of 316L stainless steel: Effects of sintering conditions on the microstructure and mechanical properties," *Additive Manufacturing,* vol. 59, p. 103147, 2022/11/01/ 2022. doi: https://doi.org/10.1016/j.addma.2022.103147

[8] D. D'Andrea, "Additive Manufacturing of AISI 316L Stainless Steel: A Review," *Metals*, vol. 13, no. 8, p. 1370. doi: https://doi.org/10.3390/met13081370

[9] D. Kong, C. Dong, X. Ni, L. Zhang, J. Yao, C. Man, X. Cheng, K. Xiao, and X. Li, "Mechanical properties and corrosion behavior of selective laser melted 316L stainless steel after different heat

treatment processes," *Journal of Materials Science & Technology,* vol. 35, no. 7, pp. 1499-1507, 2019/07/01/ 2019. doi: https://doi.org/10.1016/j.jmst.2019.03.003

[10] R. M. German, *Sintering Theory and Practice*. New York, NY, USA: Wiley, 1996.

[11] M. M. Dewidar, K. A. Khalil, and J. K. Lim, "Processing and mechanical properties of porous 316L stainless steel for biomedical applications," *Transactions of Nonferrous Metals Society of China,* vol. 17, no. 3, pp. 468-473, 2007/06/01/ 2007. doi: https://doi.org/10.1016/S1003-6326(07)60117-4

[12] R. K. Bordia, S.-J. L. Kang, and E. A. Olevsky, "Current understanding and future research directions at the onset of the next century of sintering science and technology," *Journal of the American Ceramic Society,* vol. 100, no. 6, pp. 2314-2352, 2017/06/01 2017. doi: https://doi.org/10.1111/jace.14919

[13] M. F. Modest, *Radiative Heat Transfer*. Academic Press, 2013.

[14] M. Zago, I. Cristofolini, and S. Amirabdollahian, "Designing Powder Metallurgy Process - The Influence of High Sintering Temperature on Dimensional and Geometrical Precision," in *Advances on Mechanics, Design Engineering and Manufacturing III*, Cham, 2021, pp. 3-8: Springer International Publishing. doi: https://doi.org/10.1007/978-3-030-70566-4_2

[15] C. Tosto, J. Tirillò, F. Sarasini, C. Sergi, and G. Cicala, "Fused Deposition Modeling Parameter Optimization for Cost-Effective Metal Part Printing," *Polymers*, vol. 14, no. 16, p. 3264. doi: https://doi.org/10.3390/polym14163264

[16] M. Li, J. Huang, T. Hu, B. Cheng, and H. Li, "Numerical simulation of the heating process in a vacuum sintering electric furnace and structural optimization," *Scientific Reports,* vol. 14, no. 1, p. 30905, 2024/12/28 2024. doi: https://doi.org/10.1038/s41598-024-81843-8

[17] M. F. Zaeh and M. Ott, "Investigations on heat regulation of additive manufacturing processes for metal structures," *CIRP Annals,* vol. 60, no. 1, pp. 259-262, 2011/01/01/ 2011. doi: https://doi.org/10.1016/j.cirp.2011.03.109

[18] U. Çavdar, E. Atik, M. B. Akgül, and H. Karaca, "Thermal Analyses for Induction Sintering of Powder Metal Compacts up to Sintering Temperature," *Metallofiz. Noveishie Tekhnol.,* vol. 36, no. 9, p. 1247—1258, 2014. doi: https://doi.org/10.15407/mfint.36.09.1247

[19] Y. Thompson, J. Gonzalez-Gutierrez, C. Kukla, and P. Felfer, "Fused filament fabrication, debinding and sintering as a low cost additive manufacturing method of 316L stainless steel," *Additive Manufacturing,* vol. 30, p. 100861, 2019/12/01/ 2019. doi: https://doi.org/10.1016/j.addma.2019.100861

[20] T. L. Bergman, A. S. Lavine, and F. P. Incropera, *Fundamentals of Heat and Mass Transfer*. Hoboken, NJ, USA: John Wiley & Sons, 2011.

[21] P. Restrepo-Barrientos, J. C. Maya, and M. E. Muñoz Amariles, "Modeling and Simulation of Heat Transfer in a Cold Wall Vacuum Furnace Considering Geometric Optimization of Heating Elements," in *Proceedings of the XV Ibero-American Congress of Mechanical Engineering*, Cham, 2023, pp. 271-276: Springer International Publishing. doi: https://doi.org/10.1007/978-3-031-38563-6_40

[22] R. L. Norton, *Machine Design: An Integrated Approach*. Pearson Prentice Hall, 2006.

[23] X. Chen and Y. Liu, "Design Optimization," CRC, 2018, pp. 373-418.